数理解析研究所講究録
970 巻 1996 年 125-142

The behavior of a gas in the continuum limit in the light of kinetic theory: the case of cylindrical Couette flows with evaporation and condensation

Yoshio Sone, Shigeru Takata, and Hiroshi Sugimoto

Department of Aeronautics and Astronautics, Graduate School of Engineering, Kyoto University, Kyoto 606-01, Japan

Cylindrical Couette flows of a rarefied gas between two concentric circular cylinders consisting of the condensed phase of the gas, where evaporation or condensation occurs, are considered on the basis of kinetic theory, with interest in the behavior of the gas in the continuum limit. The limiting solution is obtained by asymptotic analysis of the Boltzmann equation. In some range of the parameters of the problem, neither evaporation nor condensation occurs. The limiting solution in this case is different from the continuum solution (the conventional Couette flow without evaporation and condensation on the cylinders) and is subject to the effect of the flow that is induced if the effect of gas rarefaction is taken into account. This paradoxical result is confirmed by investigating the behavior of the numerical solution of the kinetic equation as the Knudsen number tends to zero.

I. INTRODUCTION

Recently, we studied the behavior of the temperature field in a stationary gas of the continuum limit (the limit that the mean free path of the gas molecules or the Knudsen number goes to zero) analytically and numerically on the basis of kinetic theory.[1] The result was apparently paradoxical. That is, the velocity field that would be induced by the effect of gas rarefaction (a flow of the first order of the mean free path or the Knudsen number) contributes to determination of the temperature field of the continuum limit. This is due to the fact that the Navier-Stokes set of equations (the continuity equation, momentum equations with Newton's law of stress, and energy equation with Fourier's law of heat flow), which is thought to be the fundamental set of equations of a gas of the continuum limit, contains terms of the order of the mean free path, since the viscosity and thermal conductivity of a gas are of the order of the mean free path. In the temperature problem mentioned above, the thermal creep flow[2-5] or the nonlinear thermal stress flow,[6,7] which is of the order of the mean free path, is induced except in special cases.[1] Thus, the convection term of the energy equation is of the same order of the conduction term, both of which are of the order of the mean free path, and therefore, the convection term can not be neglected. Then, one may naturally pose a question whether a similar thing can happen for a velocity field of a gas. In the present paper, we will answer this question affirmatively by taking a simple example and investigating the asymptotic solution of the Boltzmann equation for the small mean free path limit.

Consider a rarefied gas between two concentric circular cylinders consisting of the condensed phase of the gas, where each cylinder is kept at a uniform temperature and is rotating at a constant angular velocity around its axis. Let the radius, temperature, and circumferential velocity of the surface of the inner cylinder be L_1, T_1, and $V_{\theta 1}$ respectively; let the corresponding quantities of the outer cylinder be L_2, T_2, and $V_{\theta 2}$. The saturation gas pressure at temperature T (or T_1, T_2) is denoted by p_s (or p_{s1}, p_{s2}) (see Refs. 8, 9). The Knudsen number of the system is defined by l_1/L_1, where l_1 is the mean free path of the gas molecules at the equilibrium state at rest with pressure p_{s1} and temperature T_1.

When the cylinders are at rest, evaporation or condensation will take place on the inner cylinder (condensation or evaporation on the outer cylinder) according to $p_{s1} > p_{s2}$ or $p_{s1} < p_{s2}$. When either of the cylinders is rotating, the behavior of the gas may be subject to considerable change owing to pressure variation induced by the centrifugal force by the rotation of the gas. Look at the asymptotic behavior at the continuum limit ($Kn = 0_+$) of the case where $p_{s2} > p_{s1}$ and the inner cylinder is at rest. With the aid of the asymptotic theory,[10] we find that the behavior of the gas is as follows (Sec. III B): For small circumferential velocity of the outer cylinder (small $V_{\theta 2}$), evaporation takes place on the outer cylinder. As the velocity $V_{\theta 2}$ increases, the rate of evaporation decreases to vanish at some $V_{\theta 2}$, and for larger $V_{\theta 2}$, neither evaporation nor condensation occurs. In this case, the asymptotic theory in Ref. 10 is not complete to determine the limiting solution at $Kn = 0_+$ (an undetermined system), since the theory is developed for the case where the speed of evaporation or condensation is of the order of unity. One might naturally think that the flow is the conventional cylindrical Couette flow, since there is neither evaporation nor condensation. However, we will show that this is not true. In Secs. III C and III D, we derive the correct limiting solution at $Kn = 0_+$ by systematic asymptotic analysis of the boundary-value problem of the Boltzmann equation with the physical situation in mind, and show that evaporation-condensation (or a radial flow) that would be induced if the effect of gas rarefaction were taken into account contributes to determination of the behavior of the gas at $Kn = 0_+$. Finally in Sec. IV, we carry out numerical computation of the kinetic system for several small Knudsen numbers, and show that the solution approaches the limiting solution obtained in Sec. III D as the Knudsen number goes to zero.

II. BASIC EQUATION

We will investigate the cylindrical Couette flow of a rarefied gas between two cylinders consisting of the condensed phase of the gas, described in Sec. I, with a special interest of the limit of $Kn = 0_+$, under the following assumptions: (i) The behavior of the gas is described by the Boltzmann equation for hard-sphere molecules or by the Boltzmann-Krook-Welander equation[11–13]. (Formal results can be applied to general molecular models.) (ii) The velocity distribution of the gas molecules leaving the inner (or outer) cylinder is the corresponding part of the Maxwellian distribution with pressure p_{s1} (or p_{s2}), velocity $V_{\theta 1}$ (or $V_{\theta 2}$), and temperature T_1 (or T_2). This is called the complete condensation condition on the interface. However, as far as the limiting solution at $Kn = 0_+$ in the case of Secs. III C and III D, which is of main interest in the present paper, is concerned, the same solution is obtained for a more general condition, i.e., for any boundary condition that is satisfied when the velocity distribution of the gas molecules on the inner (or outer) cylinder is the Maxwellian distribution with pressure p_{s1} (or p_{s2}), velocity $V_{\theta 1}$ (or $V_{\theta 2}$), and temperature T_1 (or T_2). The weaker condition is the minimum requirement on the interface between a gas and its condensed phase; otherwise, no saturated equilibrium state exists. Thus, the limiting solution to be obtained in Sec. III D is very general. (iii) The state of the gas is circumferentially and axially uniform. Then, the axial flow velocity vanishes.

We first summarize the main notation for describing the basic equation and boundary condition. Let $\rho_{s1} = p_{s1}/RT_1$ and $k = \sqrt{\pi} Kn/2$. Then ρ_{s1} is the saturation gas density at temperature T_1. The mean free path l_1 is expressed as $l_1 = (\sqrt{2}\pi d_m^2 \rho_{s1}/m)^{-1}$ for a hard-sphere molecular gas, where d_m and m are, respectively, the diameter and mass of a molecule. With the aid of the parameters on the inner cylinder, the following nondimensional variables are introduced: $(L_1\hat{r},\ \theta,\ L_1\hat{z})$ is the cylindrical coordinate system of the physical space; $(2RT_1)^{1/2}(\zeta_r, \zeta_\theta, \zeta_z)$ is the molecular velocity in the cylindrical coordinate representation and $\boldsymbol{\zeta}$ is its vector representation; $\rho_{s1}(2RT_1)^{-3/2}\hat{\Phi}$ is the velocity distribution function of the gas molecules; $\rho_{s1}\hat{\omega}$ is the density of the gas; $(2RT_1)^{1/2}(\hat{u}_r, \hat{u}_\theta, \hat{u}_z)$, with $\hat{u}_z = 0$, is the flow velocity; $T_1\hat{\tau}$ is the temperature; $p_{s1}\hat{P}$ is the pressure; $p_{s1}\hat{P}_{ij}$ is the stress tensor; $p_{s1}(2RT_1)^{1/2}(\hat{Q}_r, \hat{Q}_\theta, \hat{Q}_z)$, with $\hat{Q}_z = 0$, is the heat-flow vector. The subscripts $\hat{r}$, θ, and $\hat{z}$ denote the radial, circumferential, and axial components respectively; the subscripts i and j in $\hat{P}_{ij}$ represent $\hat{r}$, θ, or $\hat{z}$ ($\hat{P}_{rz} = \hat{P}_{\theta z} = 0$).

With these nondimensional variables, the time-independent Boltzmann equation for hard-sphere molecules in the circumferentially and axially uniform case is written as follows:[14]

$$\zeta_r \frac{\partial \hat{\Phi}}{\partial \hat{r}} + \frac{\zeta_\theta^2}{\hat{r}} \frac{\partial \hat{\Phi}}{\partial \zeta_r} - \frac{\zeta_r \zeta_\theta}{\hat{r}} \frac{\partial \hat{\Phi}}{\partial \zeta_\theta} = \frac{1}{k} \hat{J}(\hat{\Phi}, \hat{\Phi}), \tag{1}$$

$$\hat{J}(\phi, \psi) = \frac{1}{2} \int (\phi'_* \psi' + \phi' \psi'_* - \phi_* \psi - \phi \psi_*) \hat{B}\, d\Omega(\boldsymbol{\alpha})\, d\boldsymbol{\zeta}_*, \tag{2}$$

with

$$\phi = \phi(\boldsymbol{\zeta}), \quad \phi_* = \phi(\boldsymbol{\zeta}_*), \quad \phi' = \phi(\boldsymbol{\zeta}'), \quad \phi'_* = \phi(\boldsymbol{\zeta}'_*), \quad \text{etc.},$$
$$\boldsymbol{\zeta}' = \boldsymbol{\zeta} + \boldsymbol{\alpha}[\boldsymbol{\alpha} \cdot (\boldsymbol{\zeta}_* - \boldsymbol{\zeta})], \quad \boldsymbol{\zeta}'_* = \boldsymbol{\zeta}_* - \boldsymbol{\alpha}[\boldsymbol{\alpha} \cdot (\boldsymbol{\zeta}_* - \boldsymbol{\zeta})],$$
$$\hat{B} = |\boldsymbol{\alpha} \cdot (\boldsymbol{\zeta}_* - \boldsymbol{\zeta})|/4(2\pi)^{1/2}, \qquad d\boldsymbol{\zeta}_* = d\zeta_{*r}\, d\zeta_{*\theta}\, d\zeta_{*z},$$

where $\boldsymbol{\alpha}$ is a unit vector, $d\Omega(\boldsymbol{\alpha})$ is the solid angle element in the direction of $\boldsymbol{\alpha}$, $\boldsymbol{\zeta}_*$ is the variable of integration corresponding to $\boldsymbol{\zeta}$, and the integration is carried out over the whole space of $\boldsymbol{\alpha}$ and that of $\boldsymbol{\zeta}_*$.

The complete condensation boundary condition on the cylinders is given as 12

$$\hat{\Phi} = \begin{cases} \pi^{-3/2} \exp(-\zeta_r^2 - (\zeta_\theta - \hat{v}_{\theta 1})^2 - \zeta_z^2) \quad (\zeta_r > 0) \text{ at } r = 1, \\ \hat{\sigma}_w \pi^{-3/2} \hat{\tau}_w^{-3/2} \exp(-[\zeta_r^2 + (\zeta_\theta - \hat{v}_{\theta 2})^2 + \zeta_z^2]/\hat{\tau}_w) \quad (\zeta_r < 0) \text{ at } r = L_2/L_1, \end{cases} \tag{3}$$

where

$$\hat{v}_{\theta 1} = V_{\theta 1}/(2RT_1)^{1/2}, \quad \hat{v}_{\theta 2} = V_{\theta 2}/(2RT_1)^{1/2}, \quad \hat{\sigma}_w = \rho_{s2}/\rho_{s1}, \quad \hat{\tau}_w = T_2/T_1. \tag{4}$$

The macroscopic variables $\hat{\omega}$, $\hat{u}_r$, $\hat{u}_\theta$, $\hat{\tau}$, etc. are expressed by moments of $\hat{\Phi}$:

$$\hat{\omega} = \int \hat{\Phi} d\boldsymbol{\zeta}, \tag{5a}$$

$$\hat{\omega}\hat{u}_r = \int \zeta_r \hat{\Phi} d\boldsymbol{\zeta}, \qquad \hat{\omega}\hat{u}_\theta = \int \zeta_\theta \hat{\Phi} d\boldsymbol{\zeta}, \tag{5b}$$

$$\frac{3}{2}\hat{\omega}\hat{\tau} = \int [(\zeta_r - \hat{u}_r)^2 + (\zeta_\theta - \hat{u}_\theta)^2 + \zeta_z^2] \hat{\Phi} d\boldsymbol{\zeta}, \tag{5c}$$

$$\hat{P} = \hat{\omega}\hat{\tau}, \tag{5d}$$

$$\hat{P}_{ij} = 2 \int (\zeta_i - \hat{u}_i)(\zeta_j - \hat{u}_j) \hat{\Phi} d\boldsymbol{\zeta}, \tag{5e}$$

$$\hat{Q}_r = \int (\zeta_r - \hat{u}_r)[(\zeta_r - \hat{u}_r)^2 + (\zeta_\theta - \hat{u}_\theta)^2 + \zeta_z^2] \hat{\Phi} d\boldsymbol{\zeta}, \tag{5f}$$

$$\hat{Q}_\theta = \int (\zeta_\theta - \hat{u}_\theta)[(\zeta_r - \hat{u}_r)^2 + (\zeta_\theta - \hat{u}_\theta)^2 + \zeta_z^2] \hat{\Phi} d\boldsymbol{\zeta}, \tag{5g}$$

where the integration, and in what follows unless otherwise stated, is carried out over the whole space of $\boldsymbol{\zeta}$.

For a gas with a general intermolecular potential, $\hat{B}$ in Eq. (2), which is the only quantity depending on the intermolecular potential in Eqs. (1) and (2), is a nonnegative function of $|\boldsymbol{\alpha}\cdot(\boldsymbol{\zeta}_*-\boldsymbol{\zeta})|$ and $|\boldsymbol{\zeta}_*-\boldsymbol{\zeta}|$. Further it should be noted that it contains a parameter U_0/mRT_1, where U_0 is a characteristic magnitude of the intermolecular potential. For the BKW model, which is used in Sec. IV, $\hat{J}(\hat{\Phi},\hat{\Phi})$ in Eq. (1) is expressed as

$$\hat{J}(\hat{\Phi},\hat{\Phi})=\hat{\omega}(\hat{\Phi}_e-\hat{\Phi}), \tag{6}$$

where

$$\hat{\Phi}_e=\frac{\hat{\omega}}{\pi^{3/2}\hat{\tau}^{3/2}}\exp\left(-\frac{(\zeta_r-\hat{u}_r)^2+(\zeta_\theta-\hat{u}_\theta)^2+{\zeta_z}^2}{\hat{\tau}}\right). \tag{7}$$

Corresponding to the assumption (iii), the solution $\hat{\Phi}$ of an even function of ζ_z, which is consistent with Eqs. (1) and (3), will be considered in the present paper.

III. ASYMPTOTIC ANALYSIS

A. Preliminary remarks

The asymptotic behavior for small Knudsen numbers of the solution of time-independent boundary-value problem of the Boltzmann equation in a general domain has been studied for various physical situations (e.g., Reynolds number= $o(1)$, $O(1)$, or ∞, a boundary with or without evaporation or condensation).[15–19,10] In Ref. 10, the asymptotic theory describing the behavior of a gas around a boundary consisting of condensed phase of the gas is developed, and a set of fluid dynamic equations and boundary conditions on a interface of a gas and its condensed phase is derived. The macroscopic variables of the gas in the continuum limit $Kn=0_+$ are determined by the Euler set of equations of an ideal gas. That is, in the present circumferentially and axially uniform problem,

$$\hat{\omega}\hat{u}_r\hat{r}=\text{const}, \tag{8a}$$

$$\hat{\omega}\left(\hat{u}_r\frac{d\hat{u}_r}{d\hat{r}}-\frac{\hat{u}_\theta^2}{\hat{r}}\right)=-\frac{1}{2}\frac{d\hat{P}}{d\hat{r}}, \tag{8b}$$

$$\hat{u}_r\left(\frac{d\hat{u}_\theta}{d\hat{r}}+\frac{\hat{u}_\theta}{\hat{r}}\right)=0, \tag{8c}$$

$$\hat{u}_r\frac{d}{d\hat{r}}\left(\hat{u}_r^2+\hat{u}_\theta^2+\frac{5}{2}\hat{\tau}\right)=0, \tag{8d}$$

$$\hat{P}=\hat{\omega}\hat{\tau}. \tag{8e}$$

The boundary condition on the interface is as follows: On the inner cylinder,

$$\hat{u}_\theta=\hat{v}_{\theta 1},\quad \hat{P}=\hat{h}_1(\hat{u}_r),\quad \hat{\tau}=\hat{h}_2(\hat{u}_r)\qquad [\text{if } \hat{P}<1, \text{ and } 0<\hat{u}_r\le\hat{u}_s], \tag{9a}$$

$$\hat{P}=\hat{F}_s(-\hat{u}_r,\ |\hat{u}_\theta-\hat{v}_{\theta 1}|,\ \hat{\tau})\qquad [\text{if } \hat{P}>1, \text{ and } 0<-\hat{u}_r<(5\hat{\tau}/6)^{1/2}], \tag{9b}$$

$$\hat{P}>\hat{F}_b(-\hat{u}_r,\ |\hat{u}_\theta-\hat{v}_{\theta 1}|,\ \hat{\tau})\qquad [\text{if } \hat{P}>1, \text{ and } -\hat{u}_r\ge(5\hat{\tau}/6)^{1/2}], \tag{9c}$$

where the functions $\hat{h}_1(x)$, $\hat{h}_2(x)$, and $\hat{F}_b(x,y,z)$ decrease but $\hat{F}_s(x,y,z)$ increases as x increases;[20–27] $\hat{h}_1(0_+)$, $\hat{h}_2(0_+)$, and $\hat{F}_s(0_+,y,z)$ are all equal to unity; and $\hat{u}_s$ is the positive solution of the equation $6\hat{u}_s^2-5\hat{h}_2(\hat{u}_s)=0$. On the outer cylinder,

$$\hat{u}_\theta = \hat{v}_{\theta 2}, \quad \hat{P} = \frac{p_{s2}}{p_{s1}}\hat{h}_1(-\hat{u}_r(T_1/T_2)^{1/2}), \quad \hat{\tau} = \frac{T_2}{T_1}\hat{h}_2(-\hat{u}_r(T_1/T_2)^{1/2})$$

$$[\text{if } \hat{P} < p_{s2}/p_{s1}, \text{ and } 0 < -\hat{u}_r \leq \hat{u}_s(T_2/T_1)^{1/2}], \tag{10a}$$

$$\hat{P} = \frac{p_{s2}}{p_{s1}}\hat{F}_s(\hat{u}_r(T_1/T_2)^{1/2}, |\hat{u}_\theta - \hat{v}_{\theta 2}|(T_1/T_2)^{1/2}, \hat{\tau}T_1/T_2)$$

$$[\text{if } \hat{P} > p_{s2}/p_{s1}, \text{ and } 0 < \hat{u}_r < (5\hat{\tau}/6)^{1/2}], \tag{10b}$$

$$\hat{P} > \frac{p_{s2}}{p_{s1}}\hat{F}_b(\hat{u}_r(T_1/T_2)^{1/2}, |\hat{u}_\theta - \hat{v}_{\theta 2}|(T_1/T_2)^{1/2}, \hat{\tau}T_1/T_2)$$

$$[\text{if } \hat{P} > p_{s2}/p_{s1}, \text{ and } \hat{u}_r \geq (5\hat{\tau}/6)^{1/2}]. \tag{10c}$$

The cases (9a) and (10a) correspond to evaporation on the interface; the cases (9b) and (10b) subsonic condensation; the cases (9c) and (10c) supersonic condensation. The limited range of definition in Eqs. (9a) and (10a) means that the speed of evaporation on the condensed phase cannot be supersonic.

B. The behavior of the gas at $Kn = 0_+$ I: an overview

Consider the case with $p_{s2}/p_{s1} > 1$ and $V_{\theta 1} = 0$ (or $\hat{v}_{\theta 1} = 0$). When $V_{\theta 2} = 0$ (or $\hat{v}_{\theta 2} = 0$), we obtain a radial flow evaporating from the outer cylinder as the solution of the Euler system [Eqs. (8)-(10)] (an isentropic subsonic converging flow). When the outer cylinder is rotating slowly, the flow is deformed to a spiral flow evaporating from the outer cylinder owing to Eq. (10a). However, as the speed of rotation of the outer cylinder increases, the pressure increases on the outer cylinder by the centrifugal force of the rotation of the gas, and the speed of evaporation of the gas from the outer cylinder is reduced and finally vanishes. The limiting solution as the evaporation vanishes is obtained as follows: The second factors of Eqs. (8c) and (8d) are set to be equal to zero, since the limiting solution is being looked for, and the condition (10a) on the outer cylinder is applied with $\hat{h}_1(0_+) = \hat{h}_2(0_+) = 1$ in mind. Then we have

$$\hat{u}_\theta = \frac{L_2\hat{v}_{\theta 2}}{L_1\hat{r}}, \quad \hat{\tau} = \frac{T_2}{T_1} + \frac{2\hat{v}_{\theta 2}^2}{5}\left[1 - \left(\frac{L_2}{L_1\hat{r}}\right)^2\right], \quad \hat{P}\hat{\tau}^{-5/2} = \frac{p_{s2}}{p_{s1}}\left(\frac{T_2}{T_1}\right)^{-5/2}. \tag{11}$$

The condition (9b) on the inner cylinder determines the relation among the parameters at the limiting state ($\hat{u}_r \to 0$):

$$\hat{v}_{\theta 2}^2 = \frac{5T_2}{2T_1}\left[1 - \left(\frac{p_{s2}}{p_{s1}}\right)^{-2/5}\right]\left[\left(\frac{L_2}{L_1}\right)^2 - 1\right]^{-1}. \tag{12}$$

For the higher speeds of rotation of the outer cylinder:

$$\hat{v}_{\theta 2}^2 \geq \frac{5T_2}{2T_1}\left[1 - \left(\frac{p_{s2}}{p_{s1}}\right)^{-2/5}\right]\left[\left(\frac{L_2}{L_1}\right)^2 - 1\right]^{-1}, \tag{13}$$

the solution with $\hat{u}_r = 0$ can be constructed by deforming the profiles (11) continuously. The solution is nonunique because Eqs. (8a), (8c), and (8d) degenerate and Eq. (8b) is the only remaining condition. One may consider the possibility of a flow with evaporation from the inner cylinder. The flow, if possible, is a radial isentropic flow [see Eqs. (8) and (9a) with $\hat{v}_{\theta 1} = 0$], but the flow that satisfies the boundary conditions (9a) and (10a) or (10b) is impossible.[28] In the following subsections, we develop the asymptotic theory of the Boltzmann system for small Knudsen numbers with the physical situation that $\hat{u}_r \to 0$ as $Kn \to 0$ in mind, and determine the limiting solution at $Kn = 0_+$ in the parameter range (13).

One may naturally claim that the solution is the conventional cylindrical Couette flow (the solution of the Navier-Stokes set of equations with the nonslip condition on the cylinders, where neither evaporation nor condensation occurs), since there is no radial flow, but it is not true. The analysis in the following sections gives a paradoxical result: the flow that would be induced if the effect of gas rarefaction were taken into account affects the flow of the continuum limit.

C. Asymptotic theory for the case where $\hat{u}_r \to 0$ as $Kn \to 0$

In this subsection, we develop the asymptotic theory for small Knudsen number limit of the time-independent boundary-value problem of the Boltzmann equation [Eqs. (1)-(3)] under the condition that the radial velocity vanishes in the continuum limit.

1. Fluid-dynamic type equations

Putting aside the boundary condition, we consider a moderately varying solution $[\partial\hat{\Phi}/\partial\hat{r} = O(\hat{\Phi})]$ of Eq. (1) in a power series of k. The solution is called the Hilbert solution (or expansion)[7,29–31]. That is,

$$\hat{\Phi} = \hat{\Phi}_H = \hat{\Phi}_{H0} + \hat{\Phi}_{H1}k + \cdots, \tag{14}$$

and

$$\hat{h} = \hat{h}_H = \hat{h}_{H0} + \hat{h}_{H1}k + \cdots, \tag{15}$$

where $\hat{h}$ represents any of the macroscopic variables $\hat{\omega}$, $\hat{u}_r$, $\hat{u}_\theta$, $\hat{\tau}$, etc. defined in Sec. II. By substitution of Eq. (14) into Eqs. (5a)–(5g), the component function $\hat{h}_{Hm}$ of $\hat{h}_H$ is expressed in terms of moments of $\hat{\Phi}_{Hn}$ $(n \le m)$ [note the nonlinearity of Eqs. (5b)–(5g)]. Substituting Eq. (14) into Eq. (1), we obtain the following integral equations governing the component functions $\hat{\Phi}_{Hm}$ $(m = 0, 1, \cdots)$ of the velocity distribution function $\hat{\Phi}_H$:

$$\hat{J}(\hat{\Phi}_{H0}, \hat{\Phi}_{H0}) = 0, \tag{16}$$

$$2\hat{J}(\hat{\Phi}_{H0}, \hat{\Phi}_{Hm}) = \zeta_r \frac{\partial \hat{\Phi}_{Hm-1}}{\partial \hat{r}} + \frac{\zeta_\theta^2}{\hat{r}} \frac{\partial \hat{\Phi}_{Hm-1}}{\partial \zeta_r} - \frac{\zeta_r \zeta_\theta}{\hat{r}} \frac{\partial \hat{\Phi}_{Hm-1}}{\partial \zeta_\theta} - \sum_{l=1}^{m-1} \hat{J}(\hat{\Phi}_{Hl}, \hat{\Phi}_{Hm-l}) \quad (m \ge 1). \tag{17}$$

The solution of Eq. (16) is a Maxwellian:

$$\hat{\Phi}_{H0} = \frac{\hat{\omega}_{H0}}{\pi^{3/2}\hat{\tau}_{H0}^{3/2}} \exp\left(-\frac{(\zeta_r - \hat{u}_{rH0})^2 + (\zeta_\theta - \hat{u}_{\theta H0})^2 + \zeta_z^2}{\hat{\tau}_{H0}}\right). \tag{18}$$

Equation (17) is an inhomogeneous linear integral equation for $\hat{\Phi}_{Hm}$ for $m \ge 1$. The homogeneous equation corresponding to Eq. (17) has five nontrivial solutions $\hat{\Phi}_{H0}$, $\hat{\Phi}_{H0}\zeta_r$, $\hat{\Phi}_{H0}\zeta_\theta$, $\hat{\Phi}_{H0}\zeta_z$, and $\hat{\Phi}_{H0}(\zeta_r^2 + \zeta_\theta^2 + \zeta_z^2)$. Thus, the solution of Eq. (17) is expressed in the form:[32]

$$\hat{\Phi}_{Hm} = \hat{\Phi}_{H0}\left[c_{m0} + c_{mr}\zeta_r + c_{m\theta}\zeta_\theta + c_{m4}(\zeta_r^2 + \zeta_\theta^2 + \zeta_z^2)\right] + \hat{\Psi}_{Hm} \quad (m \ge 1), \tag{19}$$

where $\hat{\Psi}_{Hm}$ is the particular solution of Eq. (17) satisfying the condition

$$\int (1, \zeta_r, \zeta_\theta, \zeta_z, \zeta_r^2 + \zeta_\theta^2 + \zeta_z^2) \hat{\Psi}_{Hm} d\boldsymbol{\zeta} = 0, \tag{20}$$

and c_{m0}, c_{mr}, $c_{m\theta}$, and c_{m4} are undetermined functions of $\hat{r}$ and related to the macroscopic variables $\hat{\omega}_{Hm}$, $\hat{u}_{rHm}$, $\hat{u}_{\theta Hm}$, and $\hat{\tau}_{Hm}$ [these variables are determined by c_{n0}, c_{nr}, $c_{n\theta}$, and c_{n4} $(n \leq m)$].

The inhomogeneous term (say, Ih_m) of Eq. (17) should satisfy the following solvability condition for Eq. (17) to have a solution, since the corresponding homogeneous equation has nontrivial solutions:

$$\int (1, \zeta_r, \zeta_\theta, \zeta_z, \zeta_r^2 + \zeta_\theta^2 + \zeta_z^2) Ih_m d\boldsymbol{\zeta} = 0, \tag{21}$$

which is reduced to

$$\int (1, \zeta_r, \zeta_\theta, \zeta_r^2 + \zeta_\theta^2 + \zeta_z^2) \left(\zeta_r \frac{\partial \hat{\Phi}_{Hm-1}}{\partial \hat{r}} + \frac{\zeta_\theta^2}{\hat{r}} \frac{\partial \hat{\Phi}_{Hm-1}}{\partial \zeta_r} - \frac{\zeta_r \zeta_\theta}{\hat{r}} \frac{\partial \hat{\Phi}_{Hm-1}}{\partial \zeta_\theta} \right) d\boldsymbol{\zeta} = 0. \tag{22}$$

In Eq. (22) the equation of ζ_z moment is omitted, because it is automatically satisfied [see Eqs. (18) and (19) with Eq.(20)]. Noting the form of Eqs. (18) and (19), we find that the partial differential equations for c_{m0}, c_{mr}, $c_{m\theta}$, and c_{m4} as well as $\hat{\omega}_{H0}$, $\hat{u}_{rH0}$, $\hat{u}_{\theta H0}$, and $\hat{\tau}_{H0}$ (or those for $\hat{\omega}_{Hm}$, $\hat{u}_{rHm}$, $\hat{u}_{\theta Hm}$, and $\hat{\tau}_{Hm}$) are derived from Eq. (22). These are the fluid-dynamic type equations.

Now we consider the Hilbert expansion under the additional condition $\hat{u}_{rH0} = 0$. The expansion can be carried out consistently under the condition.[33] Let the four solvability conditions, Eq. (22), for each m be denoted by $S_m[0]$, $S_m[r]$, $S_m[\theta]$, and $S_m[\zeta^2]$ for short. Conditions $S_1[0]$, $S_1[\theta]$, and $S_1[\zeta^2]$ are automatically satisfied. From $S_2[0]$, $S_1[r]$, $S_2[\theta]$, $S_2[\zeta^2]$, and Eq. (5d), we obtain the following differential equations for $\hat{u}_{rH1}$, $\hat{u}_{\theta H0}$, $\hat{\tau}_{H0}$, and $\hat{P}_{H0}$:

$$\frac{d\hat{\omega}_{H0}\hat{u}_{rH1}\hat{r}}{d\hat{r}} = 0, \tag{23}$$

$$\frac{\hat{\omega}_{H0}\hat{u}_{\theta H0}^2}{\hat{r}} = \frac{1}{2}\frac{d\hat{P}_{H0}}{d\hat{r}}, \tag{24}$$

$$\hat{\omega}_{H0}\hat{u}_{rH1}\left(\frac{d\hat{u}_{\theta H0}}{d\hat{r}} + \frac{\hat{u}_{\theta H0}}{\hat{r}}\right) = \frac{\gamma_1}{2\hat{r}^2}\frac{d}{d\hat{r}}\hat{\tau}_{H0}^{1/2}\hat{r}^2\left(\frac{d\hat{u}_{\theta H0}}{d\hat{r}} - \frac{\hat{u}_{\theta H0}}{\hat{r}}\right), \tag{25}$$

$$\hat{\omega}_{H0}\hat{u}_{rH1}\frac{d}{d\hat{r}}\left(\hat{u}_{\theta H0}^2 + \frac{5}{2}\hat{\tau}_{H0}\right) = \frac{\gamma_1}{\hat{r}}\frac{d}{d\hat{r}}\hat{\tau}_{H0}^{1/2}\hat{u}_{\theta H0}\hat{r}\left(\frac{d\hat{u}_{\theta H0}}{d\hat{r}} - \frac{\hat{u}_{\theta H0}}{\hat{r}}\right) + \frac{5\gamma_2}{4\hat{r}}\frac{d}{d\hat{r}}\hat{\tau}_{H0}^{1/2}\hat{r}\frac{d\hat{\tau}_{H0}}{d\hat{r}}, \tag{26}$$

$$\hat{P}_{H0} = \hat{\omega}_{H0}\hat{\tau}_{H0}, \tag{27}$$

where γ_1 and γ_2 are constants related to the collision integral (Appendix C in Ref. 1):

$$\gamma_1 = 1.270042, \quad \gamma_2 = 1.922284. \tag{28}$$

Generally, the set of conditions $S_{m+1}[0]$, $S_m[r]$, $S_{m+1}[\theta]$, and $S_{m+1}[\zeta^2]$, with the aid of the expansion form of Eq. (5d), gives the system of differential equations for $\hat{u}_{rHm}$, $\hat{u}_{\theta Hm-1}$, $\hat{\tau}_{Hm-1}$, and $\hat{P}_{Hm-1}$.

For the BKW equation, the fluid-dynamic type equations (23)–(27) need small modifications. That is, $\gamma_1 = \gamma_2 = 1$; $\hat{\tau}_{H0}^{1/2}$ on the right-hand sides of Eqs. (25) and (26) should be replaced by $\hat{\tau}_{H0}$; These changes are due to the differences of temperature dependence of transport coefficients.[34]

2. Boundary condition for the fluid-dynamic type equation

Now, we look for the solution that satisfies the boundary condition (3). The $\hat{\Phi}_{H0}$, the leading term of $\hat{\Phi}_H$, can easily be made to satisfy the condition by taking

$$\hat{u}_{\theta H0} = \hat{v}_{\theta 1}, \quad \hat{P}_{H0} = 1, \quad \hat{\tau}_{H0} = 1 \quad (\text{at } \hat{r} = 1), \tag{29a}$$

$$\hat{u}_{\theta H0} = \hat{v}_{\theta 2}, \quad \hat{P}_{H0} = p_{s2}/p_{s1}, \quad \hat{\tau}_{H0} = T_2/T_1 \quad (\text{at } \hat{r} = L_2/L_1). \tag{29b}$$

These six conditions give the boundary conditions of the differential equations (23)-(26), two first order and two second order equations. The solution of these differential equations is generally determined with the aid of the boundary conditions (29a) and (29b). It is noted that if Eqs. (29a) and (29b) are satisfied, then $\hat{\Phi}_{H0}$ satisfies the general boundary condition, which is explained in the first paragraph of Sec. II. Thus, the limiting solution is the same for the general boundary condition.

We cannot proceed the process to construct the solution that satisfies the boundary condition (3). In this process, $\hat{\Phi}_{H1}$ is required to satisfy the condition:

$$\hat{\Phi}_{H1} = 0 \quad (\text{for } \zeta_r > 0 \text{ at } \hat{r} = 1) \text{ or } (\text{for } \zeta_r < 0 \text{ at } \hat{r} = L_2/L_1). \tag{30}$$

This is impossible. In fact, $\hat{\Psi}_{H1}$ term in Eq. (19) cannot be cancelled by choosing c_{10}, $c_{1\theta}$, c_{14} (c_{1r} has already been determined with u_{rH1} in the previous stage) because of the difference of their functional dependence on $(\zeta_r, \zeta_\theta, \zeta_z)$. The solution that satisfies the boundary condition (3) can be constructed by introducing a Knudsen-layer correction that starts at the first order of the Knudsen number or k. The process of analysis is similar to that in our previous works (e.g., Refs. 15, 17–19, 1). The introduction of the Knudsen-layer correction does not affect the fluid-dynamic type equations (23)-(27) and their boundary conditions (29a) and (29b). Thus, these are the system of the equations and boundary conditions that determine the limiting solution at $Kn = 0_+$ in the case where $\hat{u}_r$ vanishes in this limit. The system presents an apparently paradoxical character: the behavior of the gas at $Kn = 0_+$ is determined together with the quantity ($\hat{u}_{rH1}$) at the order of Kn.

3. Angular momentum and energy transferred to the cylinders

The leading terms of the Knudsen-number expansion of the angular momentum AT (in the $\hat{z}$ direction) and energy ET transferred to the inner cylinder of unit axial length per unit time are, respectively, given by

$$AT = \pi^{3/2} Kn p_{s1} L_1^2 \left[\gamma_1 \frac{d}{d\hat{r}}\left(\frac{\hat{u}_{\theta H0}}{\hat{r}}\right) - \frac{2V_{\theta 1}}{(2RT_1)^{1/2}} \hat{u}_{rH1} \right]_{\hat{r}=1}, \tag{31}$$

$$ET = \pi^{3/2} Kn (2RT_1)^{1/2} p_{s1} L_1 \left[\frac{5\gamma_2}{4} \frac{d\hat{\tau}_{H0}}{d\hat{r}} + \frac{\gamma_1 V_{\theta 1}}{(2RT_1)^{1/2}} \frac{d}{d\hat{r}}\left(\frac{\hat{u}_{\theta H0}}{\hat{r}}\right) - \left(\frac{V_{\theta 1}^2}{2RT_1} + \frac{5}{2}\right) \hat{u}_{rH1} \right]_{\hat{r}=1}, \tag{32}$$

which are equal to the minus of those transferred to the outer cylinder by the laws of conservation of angular momentum and energy. In these formulas, the radial flow of the order Kn (that is, $\hat{u}_{rH1}$) plays an important role, in addition to the viscous stress and heat flow[34] determined by the quantities at $Kn = 0_+$. This reflects the fact that the viscosity and thermal conductivity of the gas are small quantities of the order of the mean free path of the gas molecules.

D. The behavior of the gas at $Kn = 0_+$ II: the case where $\hat{u}_r \to 0$ in this limit

Consider the case $p_{s2}/p_{s1} > 1$ and $V_{\theta 1} = 0$ (or $\hat{v}_{\theta 1} = 0$) with an additional condition (13). According to Sec. III B, neither evaporation nor condensation occurs on the cylinders, and there are infinitely many solutions of the Euler set of equations (8a)-(8e) with the boundary conditions (9) and (10). Here we will determine the solution of the problem as the limiting solution as $Kn \to 0$. The limiting solution is given by the solution of Eqs. (23)-(27) subject to the boundary conditions (29a) and (29b).

The differential equations (23) to (26) are reduced to the following forms by integration:

$$\hat{\omega}_{H0}\hat{u}_{rH1}\hat{r} = c_1, \tag{33}$$

$$\frac{d\hat{P}_{H0}}{d\hat{r}} = \frac{2\hat{u}_{\theta H0}^2\hat{P}_{H0}}{\hat{r}\hat{\tau}_{H0}}, \tag{34}$$

$$\frac{\gamma_1}{2}\hat{\tau}_{H0}^{1/2}\left(\frac{d\hat{u}_{\theta H0}}{d\hat{r}} - \frac{\hat{u}_{\theta H0}}{\hat{r}}\right) = \frac{c_1\hat{u}_{\theta H0}}{\hat{r}} + \frac{c_2}{\hat{r}^2}, \tag{35}$$

$$\frac{5\gamma_2}{4}\hat{\tau}_{H0}^{1/2}\frac{d\hat{\tau}_{H0}}{d\hat{r}} = \frac{5c_1\hat{\tau}_{H0}}{2\hat{r}} - \frac{2c_2\hat{u}_{\theta H0}}{\hat{r}^2} - \frac{c_1\hat{u}_{\theta H0}^2}{\hat{r}} + \frac{c_3}{r}, \tag{36}$$

where c_1, c_2, and c_3 are constants to be determined by the boundary conditions (29a) and (29b) with $\hat{v}_{\theta 1} = 0$. The constant c_1 is related to the mass flow M from the inner cylinder per unit axial length and per unit time as

$$M = \pi^{3/2}c_1\rho_{s1}(2RT_1)^{1/2}L_1 Kn, \tag{37}$$

which vanishes as $Kn \to 0$. In solving the system numerically, it is convenient to choose c_1, $\hat{v}_{\theta 2}$, T_2/T_1, and L_2/L_1 as the independent parameters of the problem instead of p_{s2}/p_{s1}, $\hat{v}_{\theta 2}$, T_2/T_1, and L_2/L_1. In doing so, we have only to treat the two equations (35) and (36), which will be solved numerically by iteration; $\hat{P}_{H0}$ (thus p_{s2}/p_{s1}) is obtained from Eq. (34) by simple integration.

Before giving the result of numerical computation, we briefly explain the solution of the system [Eqs. (33)-(36) with Eqs. (29a) and (29b)] in the limiting case where $c_1 \to \infty$ or $-\infty$. The solution is expressed by that of the system with the left-hand sides of Eqs. (35) and (36) neglected and its boundary-layer correction adjacent to the cylinder where the gas is condensing. The thickness of the boundary layer is of the order of c_1^{-1}. For $c_1 \to -\infty$, the solution is given by Eq. (11) with the boundary layer flattened on the inner cylinder (note: the replacements $\hat{u}_\theta \to \hat{u}_{\theta H0}$, $\hat{\tau} \to \hat{\tau}_{H0}$, and $\hat{P} \to \hat{P}_{H0}$ are required). The relation among the parameters p_{s2}/p_{s1}, $\hat{v}_{\theta 2}$, T_2/T_1, and L_2/L_1 when $c_1 \to -\infty$ is given by Eq. (12). For $c_1 \to \infty$, the solution is given by

$$\hat{u}_{\theta H0} = 0, \quad \hat{\tau}_{H0} = 1, \quad \hat{P}_{H0} = 1, \tag{38}$$

with the boundary layer flattened on the outer cylinder. The relation among the parameters is reduced to $p_{s2}/p_{s1} = 1$.

The range in the $(p_{s2}/p_{s1}, \hat{v}_{\theta 2})$ plane where $\hat{u}_r \to 0$ as $Kn \to 0$ [or the range given in Eq. (13)] is shown in Fig. 1 for the case T_2/T_1=1 and $L_2/L_1 = 2$, where the value of T_2/T_1 is chosen in view of the fact that the saturation pressure p_s increases very rapidly with temperature [$(T/p_s)dp_s/dT$ is large] for many kinds of gases.[35] The region, which is shaded in the figure, is the parameter range of our present interest. In the figure, curves where c_1 takes specified values are also shown. Thus we can convert the parameter c_1 to p_{s2}/p_{s1} and vice versa. The solution of the system [Eqs. (33)–(36)

with Eqs. (29a) and (29b)] is shown in Figs. 2-6 for the case $T_2/T_1 = 1$ and $L_2/L_1 = 2$. In (a) of each of Figs. 2-6, the profile of $\hat{u}_{rH1}$, $\hat{u}_{\theta H0}$, $\hat{\tau}_{H0}$, $\hat{P}_{H0}$, or $\hat{\omega}_{H0}$ at $p_{s2}/p_{s1} = 1.2$ is shown for several values of $\hat{v}_{\theta 2}$, and in (b) the profile at $\hat{v}_{\theta 2} = 0.5$ is shown for several p_{s2}/p_{s1}. The relations c_1 vs $\hat{v}_{\theta 2}$ in the case of (a) and c_1 vs p_{s2}/p_{s1} in the case of (b) are tabulated in Table I. The series (a) shows the effect of the speed of rotation, and the series (b) shows the difference of the behavior for different gases or the effect of the temperature of the cylinders for a gas, since dp_s/dT depends on temperature and thus p_{s2}/p_{s1} depends on the temperature of the cylinders.

As we have seen in Sec. III B, as the speed of rotation of the outer cylinder is increased from the rest, the evaporation from the outer cylinder decreases and vanishes at $\hat{v}_{\theta 2} = 0.2421$ [$\hat{u}_{rH0}(< 0) \to 0$] in the case of series (a) (i.e., $p_{s2}/p_{s1} = 1.2$, $T_2/T_1 = 1$, and $L_2/L_1 = 2$) [see Eq. (12)]; for larger $\hat{v}_{\theta 2}$, neither evaporation nor condensation occurs at $Kn = 0_+$. However, there is evaporation or condensation of the order of Kn [see Figure 2(a)]: at $\hat{v}_{\theta 2} = 0.2421$, $c_1 = -\infty$ (or $\hat{u}_{rH1} = -\infty$); the evaporation $-\hat{u}_{rH1}$ decreases with increase of $\hat{v}_{\theta 2}$ and vanishes at $\hat{v}_{\theta 2} = 0.6530$; for larger $\hat{v}_{\theta 2}$, the direction of evaporation and condensation is reversed, that is, evaporation of the order of Kn occurs from the inner cylinder ($\hat{u}_{rH1} > 0$) and remains at $O(Kn)$. The series (a) in Figs. 2-6 shows that the behavior of the gas at the continuum limit ($\hat{u}_{\theta H0}$, $\hat{T}_{H0}$, $\hat{P}_{H0}$, and $\hat{\omega}_{H0}$) varies considerably depending on the speed of rotation of the outer cylinder. As is obvious from Eqs. (25) and (26), this is due to the convection effect of $\hat{u}_{rH1}$ on $\hat{u}_{\theta H0}$ and $\hat{\tau}_{H0}$. This is striking from the continuum gas dynamic point of view, because something nonexisting (a rarefaction effect of gas) affects the behavior of the gas.

The series (b) of Figs. 2-6 is more convenient in comparing the present result with that of the cylindrical Couette flow without evaporation and condensation based on the continuum gas dynamics (CGD for short), since the results with the same circumferential velocity of the outer cylinder are compared for various p_{s2}/p_{s1} (or c_1). For the convenience of comparison, instead of $\hat{P}_{H0}$ and $\hat{\omega}_{H0}$ (the pressure and density normalized by p_{s1} and ρ_{s1} respectively), $\rho_{s1}\hat{P}_{H0}/\rho_{av}$ and $\rho_{s1}\hat{\omega}_{H0}/\rho_{av}$, where ρ_{av} is the average density of the gas in the domain, are shown in Figs. 5(b) and 6(b) respectively. The problem of CGD is characterized by $\hat{v}_{\theta 2}$ and T_2/T_1. Thus, all the cases shown in the series (b) from $c_1 = -\infty$ to ∞ (from $p_{s2}/p_{s1} = 2.4392$ to 1), which show a variety of profiles, correspond to a single problem in CGD. The solution of CGD coincides with that of the case $c_1 = 0$. The big differences of the profiles in Figs. 2-6 are due to $\hat{u}_{rH1}$, which is neglected in CGD.

The angular momentum AT and energy ET transferred to the inner cylinder [Eqs. (31), (32)] corresponding to the case of the series (b) of Figs. 2-6 are shown in Fig. 7. The case $c_1 = 0$ corresponds to that of CGD. In the present case, where $V_{\theta 1} = 0$, the effect of $\hat{u}_{rH1}$ is apparently absent in Eq. (31), but it enters through the profiles of $\hat{u}_{\theta H0}$ and $\hat{\tau}_{H0}$.

IV. COMPARISON WITH NUMERICAL COMPUTATION OF KINETIC EQUATION

In this section, we study the problem considered in Sec. III D by direct numerical computation of the kinetic equation for various small Knudsen numbers, and examine the behavior of the solution as the Knudsen number is getting small. This makes the paradoxical result obtained in Sec. III more persuasive. The qualitative feature of the equations for the limiting solution [Eqs. (23)-(27) and the explanation that follows] is the same for a hard-sphere molecular gas and the BKW model. Thus, we take the simpler BKW equation [Eq. (1) with Eq. (6)] as the basic equation, instead of the Boltzmann equation for hard-sphere molecules [Eq. (1) with Eq. (2)]. The boundary condition is Eq. (3).

As is pointed out in Refs. 36–38, the velocity distribution function has discontinuity in a gas around a convex body. This must be taken into account in the numerical computation. Fortunately, a finite difference system (a combination of a standard scheme and a characteristic one) is developed in a similar geometry.[37,38] We will make use of it with some modification. Thus, we do not repeat the method of computation here (see Refs. 37, 38). A point to be noted is that the asymptotic analysis in the previous section shows that a small quantity (the radial flow of the order Kn) contributes to determination of the quantities of the order unity. Thus, the accuracy of the numerical computation should be carefully examined.

The numerical computation is carried out for two typical cases in the parameter range given by Eq. (13) (this formula is independent of molecular models): case A ($\hat{v}_{\theta 2} = 0.3$, $\hat{v}_{\theta 1} = 0$, $p_{s2}/p_{s1} = 1.1$, $T_2/T_1 = 1$, and $L_2/L_1 = 2$) and case B ($\hat{v}_{\theta 2} = 0.75$, $\hat{v}_{\theta 1} = 0$, $p_{s2}/p_{s1} = 1.1$, $T_2/T_1 = 1$, and $L_2/L_1 = 2$), where $\hat{u}_r$ is supposed to be, respectively, negative and positive and to approach zero as the Knudsen number goes to zero. The velocity ($\hat{u}_r$, $\hat{u}_\theta$) of case A is shown in Fig. 8; the profile $\hat{u}_r$ and $\hat{u}_\theta$ vs $\hat{r}$ in (a), and the variation of $\hat{u}_r$ and $\hat{u}_\theta$ at some $\hat{r}$ with Kn in (b). The temperature $\hat{\tau}$ of case A is shown in Fig. 9; the profile $\hat{\tau}$ vs $\hat{r}$ in (a), and the variation of $\hat{\tau}$ at some $\hat{r}$ with Kn in (b). The corresponding figures of case B are shown in Figs. 10 and 11. The limiting solution of the BKW equation, obtained by asymptotic analysis (the method given in Sec. III D), is also shown in these figures. All figures show that the numerical solution approach the limiting solution. Obviously, it does not approach the solution of the Navier-Stokes set with the nonslip condition on the cylinders, where neither evaporation nor condensation occurs, (the solution with $c_1 = 0$), although the radial velocity $\hat{u}_r$ decreases to vanish.

V. CONCLUDING REMARKS

The interesting feature of the behavior of a gas in the continuum limit that a flow induced by the effect of gas rarefaction contributes to determination of the behavior of a gas in the continuum limit is not special to the present problem. As mentioned in Sec. I, it comes from the fact that the viscous and heat-conduction terms in the Navier-Stokes set of equations are of the order of the mean free path (or Knudsen number), since viscosity and thermal conductivity of a gas are of that order. Thus these terms are generally small and can be neglected except in the viscous and thermal boundary layers and a shock layer.[39–41] There are various cases, with flow or without flow, where the convection terms vanish in some of the momentum equations or in the energy equation. In these equations, viscous and conduction terms, which are of the order of Kn, become important. On the other hand, various types of flows, as the present flow or flows induced by a temperature field,[2–7,42,43] are induced if the effect of gas rarefaction is taken into account. Then convection terms of the order Kn may revive in some of the momentum equations or in the energy equation, and balance with the viscous or conduction term. The convection term in the energy equation revives in the problem treated in Ref. 1, and some convection terms revive in the θ component of the momentum equations and in the energy equation in the present problem. Thus something nonexisting in the sense of CGD (a flow induced by the effect of gas rarefaction) contributes to determination of the behavior of a gas in the continuum limit. In the present problem the fluid-dynamic type equations derived in Sec. III C are practically the Navier-Stokes set of equations, but in the case of Ref. 1 it contains thermal stress terms, which are outside the framework of the

Navier-Stokes set. In order to obtain the correct fluid-dynamic type equations and their associate boundary conditions, it is required to carry out systematic asymptotic analysis of the kinetic system (a boundary-value problem of the Boltzmann equation) by paying attention to the order of the magnitude of the physical variables in the problem under consideration. Finally, it is noted that rarefied gas dynamic consideration is required even in the study of a gas in the continuum limit.

REFERENCES

[1] Y. Sone, K. Aoki, S. Takata, H. Sugimoto, and A. V. Bobylev, Phys. Fluids A **8**, 628 (1996).

[2] E. H. Kennard, *Kinetic Theory of Gases* (McGraw-Hill, New York, 1938), p. 327.

[3] L. Loeb, *Kinetic Theory of Gases* (Dover, New York, 1961), Secs. 83, 84.

[4] Y. Sone, J. Phys. Soc. Jpn. **21**, 1836 (1966).

[5] T. Ohwada, Y. Sone, and K. Aoki, Phys. Fluids A **1**, 1588 (1989).

[6] M. N. Kogan, V. S. Galkin, and O. G. Fridlender, Sov. Phys. Usp. **19**, 420 (1976).

[7] Y. Sone and K. Aoki, *Molecular Gas Dynamics* (Asakura, Tokyo, 1994), Chap. 3 (in Japanese).

[8] L. Landau and E. Lifchitz, *Statistical Physics, Part I* (Pergamon Press, Oxford, 1980), Chap. VIII.

[9] F. Reif, *Fundamentals of Statistical and Thermal Physics* (McGraw-Hill, New York, 1965), p. 304.

[10] K. Aoki and Y. Sone, in *Advances in Kinetic Theory and Continuum Mechanics*, edited by R. Gatignol and Soubbaramayer (Springer-Verlag, Berlin, 1991), p. 43.

[11] P. L. Bhatnagar, E. P. Gross, M. Krook, Phys. Rev., **94**, 511 (1954).

[12] P. Welander, Ark. Fys., **7**, 507(1954).

[13] M. N. Kogan, Appl. Math. Mech. **22**, 597 (1958).

[14] M. N. Kogan, *Rarefied Gas Dynamics* (Plenum, New York, 1969), Appendix 1.

[15] Y. Sone, in *Rarefied Gas Dynamics*, edited by L. Trilling and H. Y. Wachman (Academic, New York, 1969), Vol. 1, p. 243.

[16] J. S. Darrozes, in *Rarefied Gas Dynamics*, edited by L. Trilling and H. Y. Wachman (Academic, New York, 1969), Vol. 1, p. 111.

[17] Y. Sone, in *Rarefied Gas Dynamics*, edited by D. Dini (Editrice Tecnico Scientifica, Pisa, 1971), Vol. 2, p. 737.

[18] Y. Sone and K. Aoki, Transp. Theory Stat. Phys. **16**, 189 (1987).

[19] Y. Sone, in *Advances in Kinetic Theory and Continuum Mechanics*, edited by R. Gatignol and Soubbaramayer (Springer-Verlag, Berlin, 1991), p. 19.

[20] This statement is not a mathematical theorem, but a conjecture formed on the basis of various numerical computations.[21–27]. The detailed numerical data of these functions for the BKW equation are found in Ref. 27. It is noted that the Mach numbers corresponding to $\hat{u}_r$ and $\hat{u}_\theta$ are used there instead of them.

[21] T. Ytrehus, in *Rarefied Gas Dynamics*, edited by J. L. Potter (AIAA, New York, 1977), p. 1197.

[22] Y. Sone, K. Aoki, and I. Yamashita, in *Rarefied Gas Dynamics*, edited by V. Boffi and C. Cercignani (Teubner, Stuttgart, 1986), Vol. 2, p. 323.

[23] Y. Sone and H. Sugimoto, in *Adiabatic Waves in Liquid-Vapor Systems*, IUTAM Symposium, Göttingen, 1989, edited by G. E. A. Meier and P. A. Thompson (Springer, Berlin, 1990), p. 293.

[24] M. N. Kogan and A. A. Abramov, in *Rarefied Gas Dynamics*, edited by A. E. Beylich (VCH, Weinheim, 1991), p. 1251.

[25] A. P. Kryukov, in *Rarefied Gas Dynamics*, edited by A. E. Beylich (VCH, Weinheim, 1991), p. 1278.

[26] K. Aoki, Y. Sone, and T. Yamada, Phys. Fluids A **2**, 1867 (1990) .

[27] K. Aoki, K. Nishino, Y. Sone, and H. Sugimoto, Phys. Fluids A **3**, 2260 (1991).

[28] The nonexistence can be shown without knowing the exact values of the functions $\hat{h}_1$, $\hat{h}_2$, $\hat{F}_s$, and $\hat{F}_b$ in Eqs. (8) and (9). These functions are determined by the analysis of the half space boundary-value problem of the Boltzmann equation. From the H theorem applied to the half space problem, with the aid of the conservation relations, we obtain the following inequality on $\hat{h}_1$: $\hat{h}_1 \leq \hat{h}_2^{5/2} \exp(-\hat{u}_i^2 + 5(1-\hat{h}_2)/2)$. With this inequality, no flow evaporating from the inner cylinder is found to be possible when $p_{s2}/p_{s1} > 1$ [For a supersonic flow, the relation between $\hat{F}_s$ and $\hat{F}_b$ mentioned in Ref. 27 is used]. The details of this discussion will be given elsewhere.

[29] D. Hilbert, *Grundzuge einer Allgemeinen Theorie der Linearen Integralgleichungen* (Teubner, Wien, 1924), Chap. 22.

[30] H. Grad, in *Handbuch der Physik*, edited by S. Flügge (Springer-Verlag, Berlin, 1958), Band XII, p. 205.

[31] C. Cercignani, *The Boltzmann Equation and Its Applications* (Springer-Verlag, Berlin, 1988), Chap. V.

[32] A solution with $\hat{u}_z = 0$ is considered in this paper.

[33] This is seen from the fact that the condition $\hat{u}_{rH0} = 0$ is consistent with the Euler set (8a)-(8d).

[34] The nondimensional stress $\hat{P}_{r\theta}$ and heat flow $\hat{Q}_r$ are given as follows: for a hard-sphere molecular gas, $\hat{P}_{r\theta H0} = 0$, $\hat{P}_{r\theta H1} = -\gamma_1 \hat{\tau}_{H0}^{1/2} \hat{r} d(\hat{r}^{-1}\hat{u}_{\theta H0})/dr$; $\hat{Q}_{rH0} = 0$, $\hat{Q}_{rH1} = -(5/4)\gamma_2 \hat{\tau}_{H0}^{1/2} d\hat{\tau}_{H0}/d\hat{r}$; for the BKW model, $\hat{\tau}_{H0}^{1/2}$ in the formulas is to be replaced by $\hat{\tau}_{H0}$. No Knudsen-layer correction is required up to this order.

[35] For many kinds of gases far away from their critical point, $(T/p_s)dp_s/dT > 10$. Thus $T_2/T_1 < 1.02$ when $p_{s2}/p_{s1} = 1.2$, for example.

[36] Y. Sone and S. Takata, Transp. Theory Stat. Phys. **21**, 501 (1992).

[37] H. Sugimoto and Y. Sone, Phys. Fluids A **4**, 419 (1992).

[38] Y. Sone and H. Sugimoto, Phys. Fluids **7**, 2072 (1995).

[39] A shock layer, except a weak one, cannot correctly be described by the Navier-Stokes set. Analysis by kinetic theory is required for its correct description.

[40] H. Grad, in *Transport Theory*, edited by R. Bellman, G. Birkhoff, and I. Abu-Shumays (American Mathematical Society, Providence, 1969), p. 269.

[41] C. Cercignani and C. Lancellotti, in *Rarefied Gas Dynamics*, edited by A. E. Beylich (VCH, Weinheim, 1991), p. 153.

[42] M. N. Kogan, Prog. Aerospace Sci. **29**, 271 (1992).

[43] K. Aoki, Y. Sone, and N. Masukawa, in *Rarefied Gas Dynamics*, edited by J. Harvey and G. Lord (Oxford Univ. Press, Oxford, 1995), Vol. I, p. 35.

Table I. The relations c_1 vs $\hat{v}_{\theta 2}$ with $p_{s2}/p_{s1} = 1.2$ and c_1 vs p_{s2}/p_{s1} with $\hat{v}_{\theta 2} = 0.5$ in the case $\hat{v}_{\theta 1} = 0$, $T_2/T_1 = 1$, and $L_2/L_1 = 2$.

$p_{s2}/p_{s1} = 1.2$		$\hat{v}_{\theta 2} = 0.5$	
c_1	$\hat{v}_{\theta 2}$	c_1	p_{s2}/p_{s1}
∞	∞	∞	1.0000
10	1.5094	10	1.0219
5	1.1021	5	1.0399
1	0.7377	1	1.0886
0	0.6530	0	1.1136
−1	0.5771	−1	1.1469
−5	0.3850	−5	1.3662
−10	0.3059	−10	1.6637
$-\infty$	0.2421	$-\infty$	2.4392

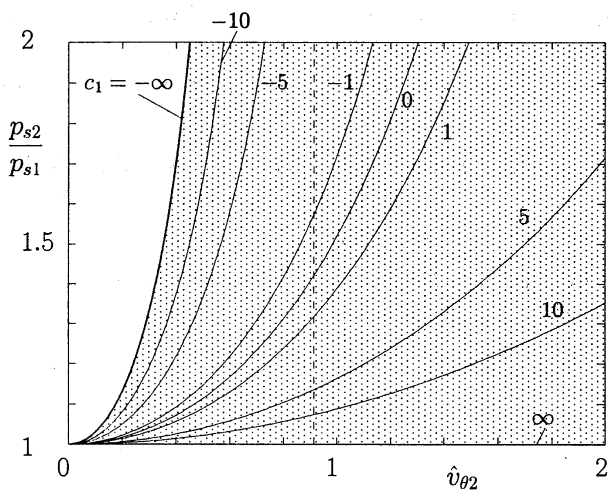

Fig. 1 Classification of solutions on the ($\hat{v}_{\theta 2}$, p_{s2}/p_{s1}) plane in the case ($\hat{v}_{\theta 1} = 0$, $T_2/T_1 = 1$, and $L_2/L_1 = 2$). The shaded part is the region where $\hat{u}_r \to 0$ as $Kn \to 0$ [see Eq. (13)]; —— is the curve $c_1 = \text{const}$ [see Eqs. (37) and (38)]; - - - - is the asymptote ($\hat{v}_{\theta 2} = \sqrt{5/6}$) of the curve $c_1 = -\infty$.

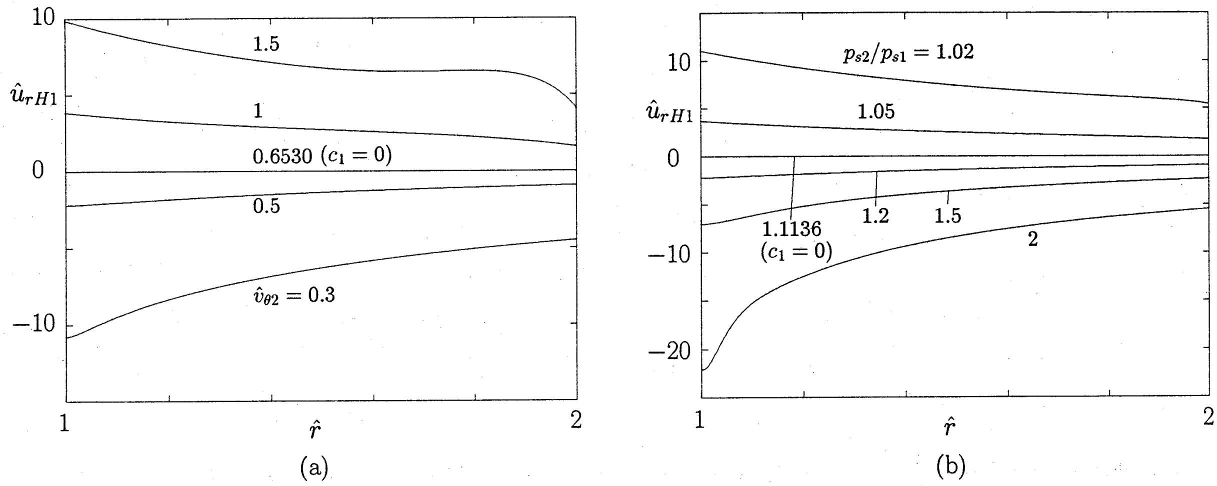

Fig. 2 Radial velocity profiles $\hat{u}_{rH1}$ vs $\hat{r}$. (a) The profiles for various $\hat{v}_{\theta 2}$ in the case $\hat{v}_{\theta 1} = 0$, $p_{s2}/p_{s1} = 1.2$, $T_2/T_1 = 1$, and $L_2/L_1 = 2$; (b) the profiles for various p_{s2}/p_{s1} (or c_1) in the case $\hat{v}_{\theta 1} = 0$, $\hat{v}_{\theta 2} = 0.5$, $T_2/T_1 = 1$, and $L_2/L_1 = 2$.

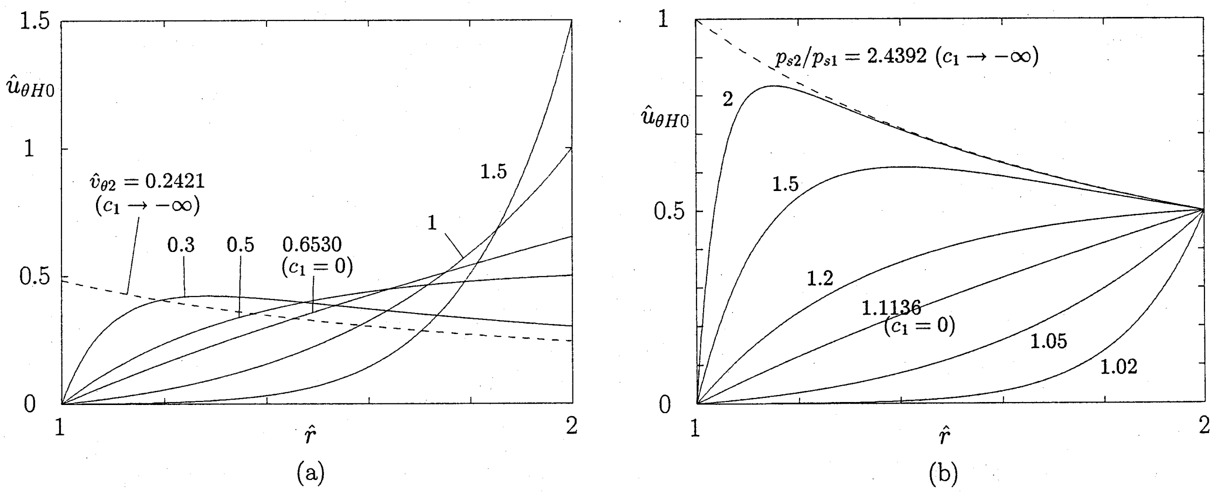

Fig. 3 Circumferential velocity profiles $\hat{u}_{\theta H0}$ vs $\hat{r}$. (a) The profiles for various $\hat{v}_{\theta 2}$ in the case $\hat{v}_{\theta 1} = 0$, $p_{s2}/p_{s1} = 1.2$, $T_2/T_1 = 1$, and $L_2/L_1 = 2$; (b) the profiles for various p_{s2}/p_{s1} (or c_1) in the case $\hat{v}_{\theta 1} = 0$, $\hat{v}_{\theta 2} = 0.5$, $T_2/T_1 = 1$, and $L_2/L_1 = 2$.

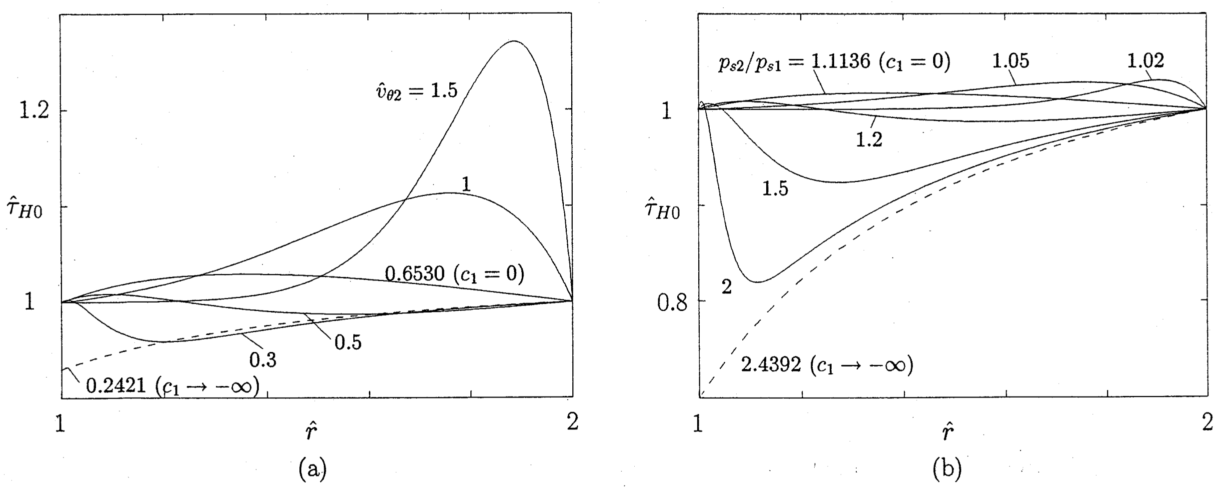

Fig. 4 Temperature profiles $\hat{\tau}_{H0}$ vs $\hat{r}$. (a) The profiles for various $\hat{v}_{\theta 2}$ in the case $\hat{v}_{\theta 1} = 0$, $p_{s2}/p_{s1} = 1.2$, $T_2/T_1 = 1$, and $L_2/L_1 = 2$; (b) the profiles for various p_{s2}/p_{s1} (or c_1) in the case $\hat{v}_{\theta 1} = 0$, $\hat{v}_{\theta 2} = 0.5$, $T_2/T_1 = 1$, and $L_2/L_1 = 2$.

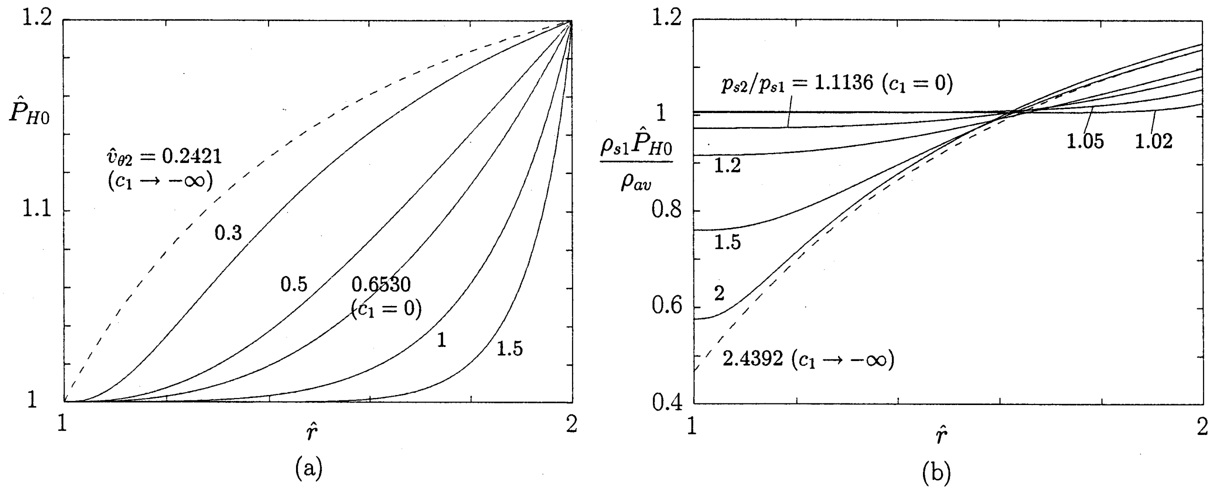

Fig. 5 Pressure profiles. (a) The profiles $\hat{P}_{H0}$ vs $\hat{r}$ for various $\hat{v}_{\theta 2}$ in the case $\hat{v}_{\theta 1} = 0$, $p_{s2}/p_{s1} = 1.2$, $T_2/T_1 = 1$, and $L_2/L_1 = 2$; (b) the profiles $\rho_{s1}\hat{P}_{H0}/\rho_{av}$ vs $\hat{r}$ for various p_{s2}/p_{s1} (or c_1) in the case $\hat{v}_{\theta 1} = 0$, $\hat{v}_{\theta 2} = 0.5$, $T_2/T_1 = 1$, and $L_2/L_1 = 2$.

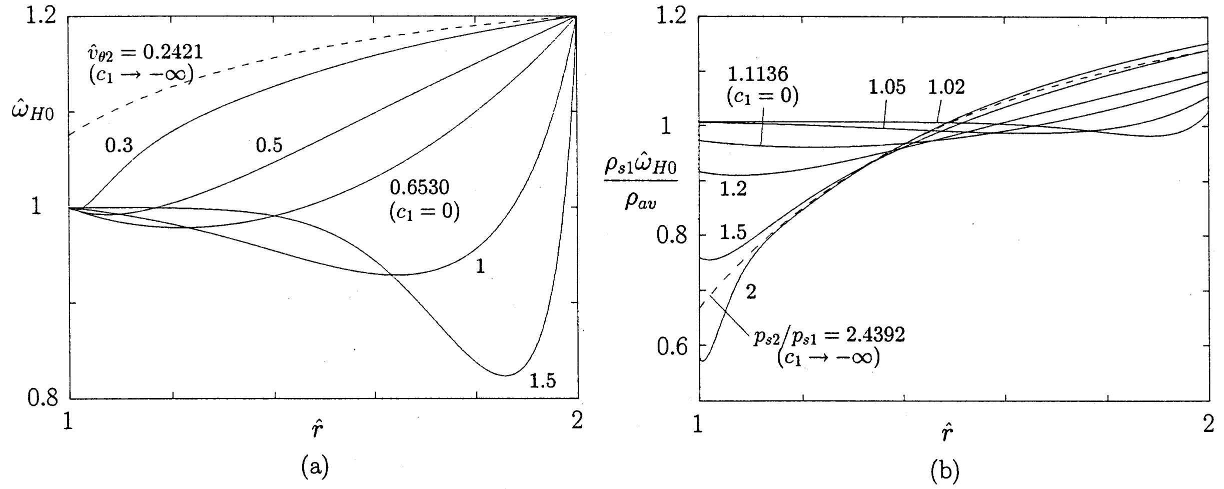

Fig. 6 Density profiles. (a) The profiles $\hat{\omega}_{H0}$ vs $\hat{r}$ for various $\hat{v}_{\theta 2}$ in the case $\hat{v}_{\theta 1} = 0$, $p_{s2}/p_{s1} = 1.2$, $T_2/T_1 = 1$, and $L_2/L_1 = 2$; (b) the profiles $\rho_{s1}\hat{\omega}_{H0}/\rho_{av}$ vs $\hat{r}$ for various p_{s2}/p_{s1} (or c_1) in the case $\hat{v}_{\theta 1} = 0$, $\hat{v}_{\theta 2} = 0.5$, $T_2/T_1 = 1$, and $L_2/L_1 = 2$.

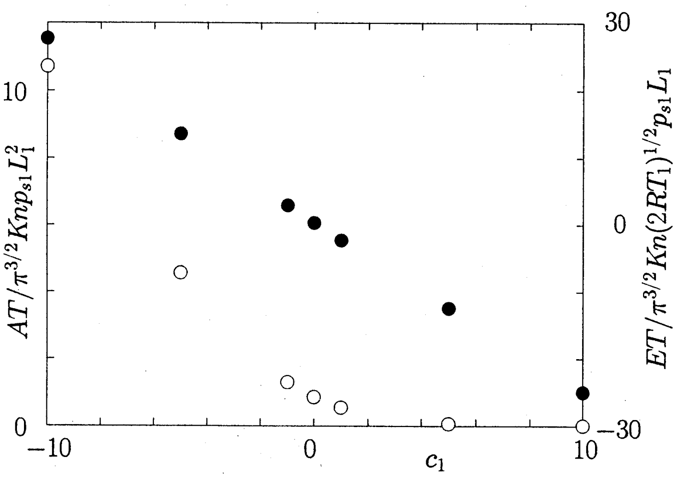

Fig. 7 Angular momentum AT and energy ET transferred to the inner cylinder [Eqs. (31) and (32)] as functions of c_1 in the case $\hat{v}_{\theta 1} = 0$, $\hat{v}_{\theta 2} = 0.5$, $T_2/T_1 = 1$ and $L_2/L_1 = 2$. Here, ○: $AT/\pi^{3/2}Knp_{s1}L_1^2$, ●: $ET/\pi^{3/2}Kn(2RT_1)^{1/2}p_{s1}L_1$.

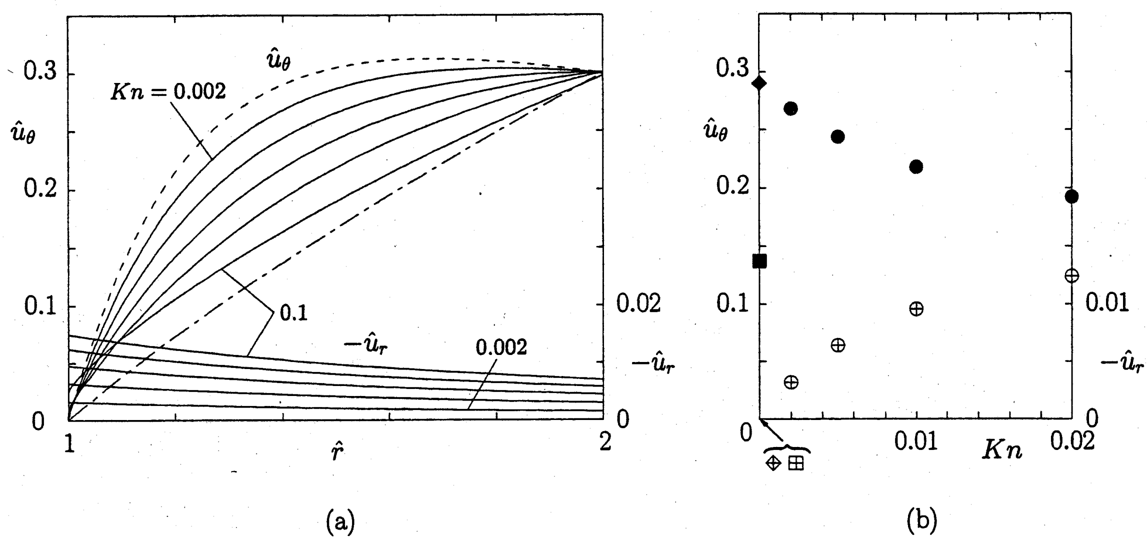

Fig. 8 Comparison of the numerical solution of the BKW equation for small Kn with the corresponding limiting solution obtained by the asymptotic analysis in Sec. III D for case A ($\hat{v}_{\theta 1} = 0$, $\hat{v}_{\theta 2} = 0.3$, $p_{s2}/p_{s1} = 1.1$, $T_2/T_1 = 1$, and $L_2/L_1 = 2$) I: the flow velocity field. (a) The profiles $\hat{u}_r$ vs $\hat{r}$ and $\hat{u}_\theta$ vs $\hat{r}$; (b) the variations of $\hat{u}_r$ at $\hat{r} = 1$ and $\hat{u}_\theta$ at $\hat{r} = 1.4$ with Kn. Here —— in (a) and the circles ●, ⊕ in (b): numerical solution; - - - - in (a) and the diamonds ♦, ◈ in (b): asymptotic theory; — - — in (a) and the squares ■, ⊞ in (b): CGD (the solution without evaporation-condensation of the Navier-Stokes equation under the nonslip condition, where the viscosity and thermal conductivity derived from the BKW equation are taken). The black symbols ●, ♦, ■ in (b): $\hat{u}_\theta$ at $\hat{r} = 1.4$; the symbols with cross ⊕, ◈, ⊞ in (b): $\hat{u}_r$ at $\hat{r} = 1$. The numerical solution in a solid line in (a) is given for five Knudsen numbers (Kn=0.002, 0.005, 0.01, 0.02, 0,1). Only the curves for Kn=0.002 and 0.1 are labeled; the other curves are located in the order of the magnitude of Kn and thus easily identified. Note the difference of the scales of $\hat{u}_r$ and $\hat{u}_\theta$.

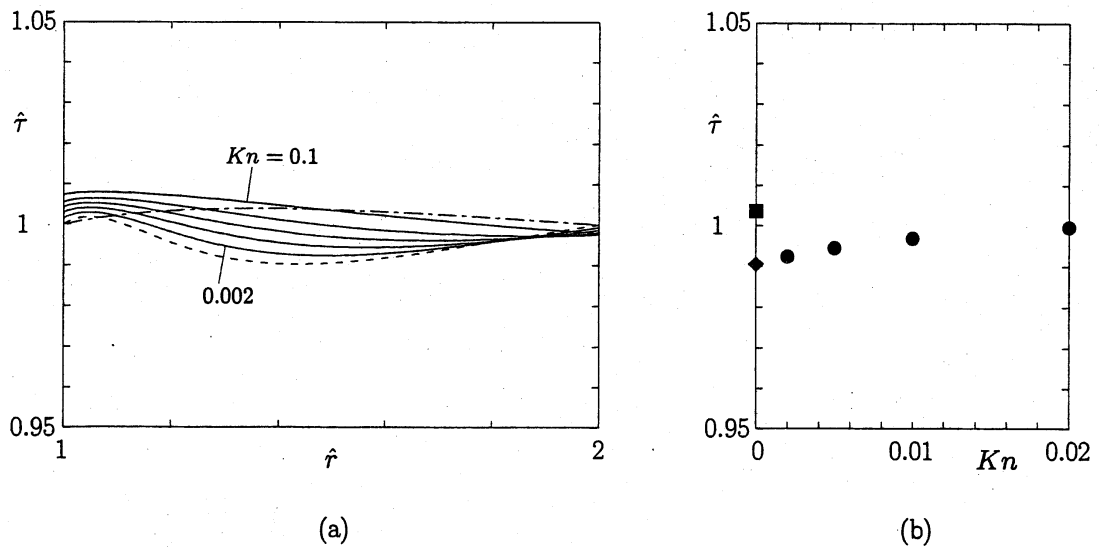

Fig. 9 Comparison of the numerical solution of the BKW equation for small Kn with the corresponding limiting solution obtained by the asymptotic analysis in Sec. III D for case A ($\hat{v}_{\theta 1} = 0$, $\hat{v}_{\theta 2} = 0.3$, $p_{s2}/p_{s1} = 1.1$, $T_2/T_1 = 1$, and $L_2/L_1 = 2$) II: the temperature field. (a) The profile $\hat{\tau}$ vs $\hat{r}$; (b) the variation of $\hat{\tau}$ at $\hat{r} = 1.5$ with Kn. Here —— in (a) and the circle ● in (b): numerical solution; - - - - in (a) and the diamond ♦ in (b): asymptotic theory; — - — in (a) and the square ■ in (b): CGD (see the caption of Fig. 8). The numerical solution in a solid line in (a) is given for five Knudsen numbers (Kn=0.002, 0.005, 0.01, 0.02, 0,1). Only the curves for Kn=0.002 and 0.1 are labeled; the other curves are located in the order of the magnitude of Kn and thus easily identified.

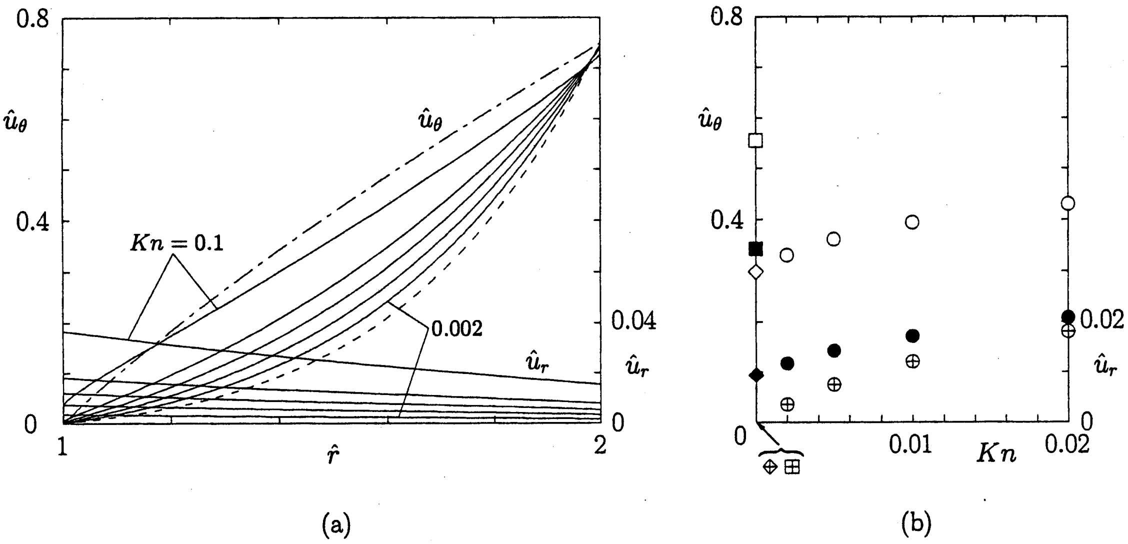

Fig. 10 Comparison of the numerical solution of the BKW equation for small Kn with the corresponding limiting solution obtained by the asymptotic analysis in Sec. III D for case B ($\hat{v}_{\theta 1} = 0$, $\hat{v}_{\theta 2} = 0.75$, $p_{s2}/p_{s1} = 1.1$, $T_2/T_1 = 1$. and $L_2/L_1 = 2$) I: the flow velocity field. (a) The profiles $\hat{u}_r$ vs $\hat{r}$ and $\hat{u}_\theta$ vs $\hat{r}$; (b) the variations of $\hat{u}_r$ at $\hat{r} = 1$ and $\hat{u}_\theta$ at $\hat{r} = 1.4$ and 1.7 with Kn. Here, —— in (a) and the circles ●, ○, ⊕ in (b): numerical solution; - - - - in (a), the diamonds ◆, ◇, ⟠ in (b): asymptotic theory; — - — in (a) and the squares ■, □, ⊞ in (b): CGD (see the caption of Fig. 8). The black symbols ●, ◆, ■ in (b): $\hat{u}_\theta$ at $\hat{r} = 1.4$; the white ones ○, ◇, □ in (b): $\hat{u}_\theta$ at $\hat{r} = 1.7$; the symbols with cross ⊕, ⟠, ⊞ in (b): $\hat{u}_r$ at $\hat{r} = 1$. Note the difference of the scales of $\hat{u}_r$ and $\hat{u}_\theta$. The numerical solution in a solid line in (a) is given for five Knudsen numbers (Kn=0.002, 0.005, 0.01, 0.02, 0,1). Only the curves for Kn=0.002 and 0.1 are labeled; the other curves are located in the order of the magnitude of Kn and thus easily identified.

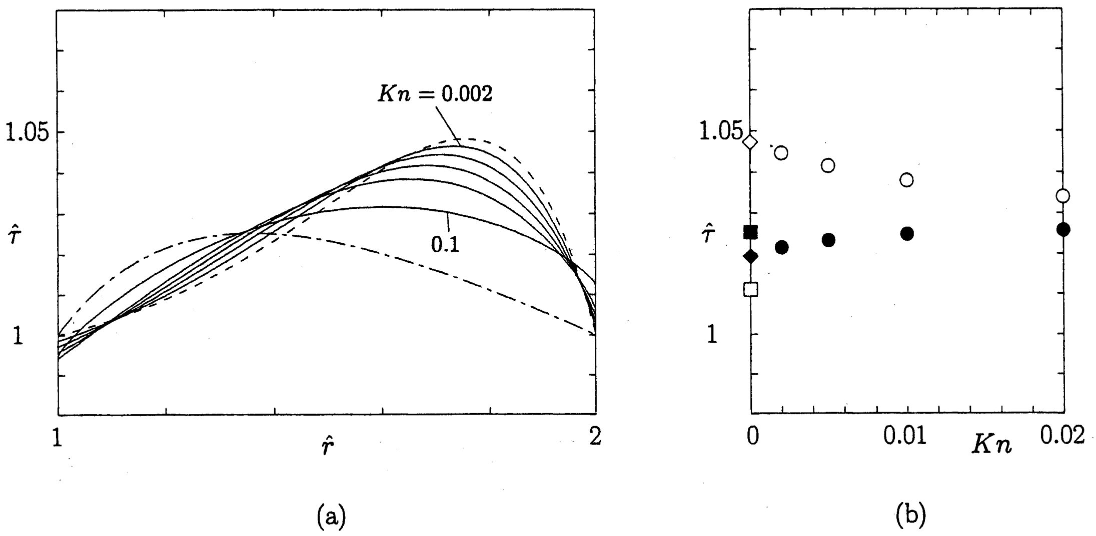

Fig. 11 Comparison of the numerical solution of the BKW equation for small Kn with the corresponding limiting solution obtained by the asymptotic analysis in Sec. III D for case B ($\hat{v}_{\theta 1} = 0$, $\hat{v}_{\theta 2} = 0.75$, $p_{s2}/p_{s1} = 1.1$, $T_2/T_1 = 1$, and $L_2/L_1 = 2$) II: the temperature field. (a) The profile $\hat{T}$ vs $\hat{r}$; (b) the variations of $\hat{T}$ at $\hat{r} = 1.35$ and 1.8 with Kn. Here —— in (a) and the circles ●, ○ in (b): numerical solution; - - - - in (a) and the diamonds ◆, ◇ in (b): asymptotic theory; — - — in (a) and the squares ■, □: CGD (see the caption of Fig. 8). The black symbols ●, ◆, ■: $\hat{T}$ at $\hat{r} = 1.35$; the white ones ○, ◇, □: $\hat{T}$ at $\hat{r} = 1.8$. The numerical solution in a solid line in (a) is given for five Knudsen numbers (Kn=0.002, 0.005, 0.01, 0.02, 0,1). Only the curves for Kn=0.002 and 0.1 are labeled; the other curves are located in the order of the magnitude of Kn and thus easily identified.